

User's Guide for GOES-R XRS L2 Products

Janet Machol, Stefan Codrescu and Courtney Peck

9 July 2024

Contents

1	Summary	2
2	XRS L2 Products Overview	2
2.1	Science Quality versus Operational XRS Data	3
2.2	Flare Magnitudes	3
2.3	XRS Response Functions	4
2.4	Time	4
2.5	Related New Data Products	5
3	1-second Irradiances Product	5
4	1-minute Averages Product	5
5	Flare Summary and Flare Detection Products	7
6	Flare Location Product	8
7	Daily Background Product	9
8	Plots	9
9	Acknowledgements	11
10	References	11
A	Flare Detection Algorithm	12
A.1	Flare Detection Algorithm	12
A.2	Algorithm Steps	13
A.2.1	(Steps 1-6) Prepare data and do simple comparisons	14
A.2.2	(Steps 8a-f) Check for start of flare	14
A.2.3	(Steps 9a-c) Rising flare	15
A.2.4	(Steps 10a-b) Declining flare	15
A.2.5	(Steps 11a-e) Final steps to exit	16
A.3	Algorithm Inputs	16
B	Flare Location Algorithm	18
C	Daily Background Algorithm	20

1 Summary

The GOES X-Ray Sensor (XRS) measurements have been a crucial component of space weather operations since 1975, providing an accurate measurement of geoeffective X-ray irradiance from second-to-second real-time conditions to solar-cycle time scales (Garcia, 1994). XRS measurements are in two bandpass channels commonly referred to as the XRS-A (0.05-0.4 nm) and XRS-B (0.1-0.8 nm), both of which are in the soft X-ray portion of the electromagnetic spectrum. This User’s Guide discusses the algorithms used to generate the GOES-R XRS L2 data products.

The GOES-R XRS instrument provides irradiance ranges of more than 6 orders of magnitude by using two photodiode sets to cover overlapping portions of the irradiance range for the XRS-A channel and also for the XRS-B channel. XRS-A1 and XRS-B1 are larger Si diodes used to measure low X-ray fluxes, and XRS-A2 and XRS-B2 are smaller, quadrant Si diodes used to measure high X-ray fluxes, and to also provide approximate flare location on the solar disk. For each 1-s measurement, one of the A channels and one of the B channels are designated as the primary channels depending on the measured irradiance and channel switching threshold. Use of the primary channel avoids issues at low fluxes where the XRS-A2 and -B2 channels are not sensitive, and at very high fluxes, where the XRS-A1 and -B1 diodes saturate. The XRS instrument is described in detail by Chamberlin et al. (2009). On the GOES-R series satellites, XRS is part of the Extreme Ultraviolet and X-Ray Irradiance Sensors (EXIS). EXIS was designed and built by the Laboratory for Atmospheric and Space Physics (LASP) at the University of Colorado Boulder.

For XRS, the Level 2 (L2) data consists of cleaned 1-s data and higher order products such as irradiance averages, flare event summaries, and flare location. The 1-minute integrated XRS-B irradiance is used for solar flare classifications, and is key to NOAA Space Weather Prediction Center (SWPC) operations, allowing early warnings of major flares to be issued. Due to the Neupert effect (Neupert, 1968), during a solar flare, the harder X-rays measured by XRS-A reach their maximum value in advance of the softer XRS-B X-rays. The ratio of the XRS-A to -B irradiance has a variety of uses including the issuance of alerts by the SWPC forecasters, calculations of the flare temperature (e.g., Woods et al., 2008), and the derivation of the mean solar coronal temperature during non-flare conditions (Thomas et al., 1985; Garcia, 1994; White et al., 2005). The flare summary files can have a number of practical and scientific applications, such as determining the total energy input to the ionosphere’s D-region.

Science-quality XRS L1b and L2 netCDF datasets are produced by NOAA’s National Center for Environmental Information (NCEI), and differ from the operational products used at SWPC in that the data have been reprocessed from the start of the mission to the present date and incorporate retrospective fixes for issues and outages in the operational product (see Section 2.1). Users are advised to use the science quality data XRS L2 data instead of the operational data. The science quality data directories have names which end in “_science” and the file names have prefixes of “sci”.

This User’s Guide gives details of the GOES-R XRS L2 algorithms. Users of the GOES-R XRS data are responsible for inspecting the data and understanding the known caveats prior to use. Data caveats are given in the GOES-R XRS Science Quality L2 Readme. Links to the science-quality XRS data, Readme’s, a User’s Guide, plots, responsivity data, and associated documentation can be found at <https://www.ngdc.noaa.gov/stp/satellite/goes-r.html>. Technical questions about this data can be sent to janet.machol@noaa.gov, while questions about data access should be sent to pamela.wyatt@noaa.gov or josh.riley@noaa.gov.

2 XRS L2 Products Overview

XRS measures soft X-ray fluxes at 1-second cadence in the historical bandpasses of 0.05 to 0.4 nm and 0.1 to 0.8 nm, corresponding to Channels XRS-A and -B, respectively. Each channel has two irradiance sensors to capture the full dynamic range of the solar X-ray irradiance, where “1” denotes the low-irradiance sensor and “2” is for the high-irradiance sensor. This numbering is utilized in the variable naming where, for example, “xrsa2_flux” corresponds to the irradiance in Channel A on the high irradiance sensor. The flag “xrsa_primary_chan” indicates whether XRS-A1 or XRS-A2 provides the primary irradiance values and for each channel, the value from the selected primary sensor is available in the “xrsa_flux” or “xrsb_flux” variable. The current thresholds for switching the primary channels are 10^{-5} W m⁻² for Channel A and 10^{-4} W m⁻² for Channel B. The terms irradiance and flux are used interchangeably in this document.

Figure 1 shows measurement time periods for the three GOES satellites. The six L2 products for XRS are listed in Table 1.

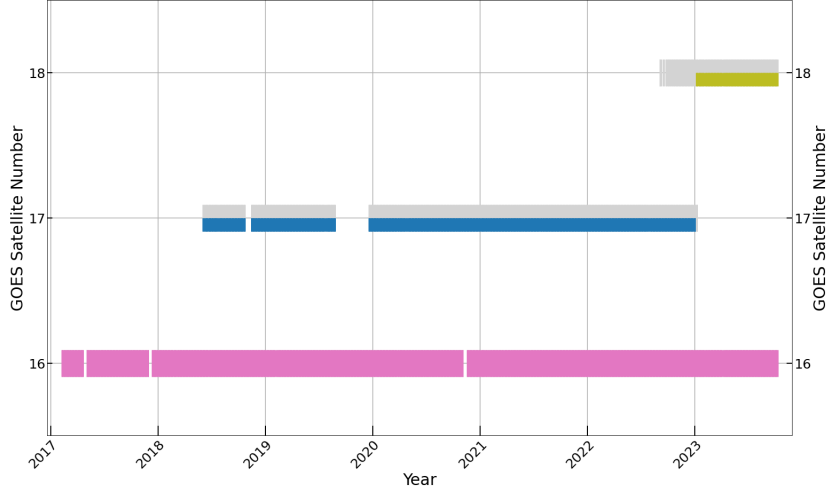


Figure 1: XRS measurements for GOES-16 through -18 as of December 2023. Coloring indicates primary (full-thickness lines) and secondary (half-thickness lines) satellites.

Table 1: Summary of XRS L2 Products

Product	Name	Description
1s fluxes	flx1s	XRS irradiances at 1-s cadence
1-min fluxes	avg1m	XRS irradiances at 1-min cadence
flare summary	flsum	flare detection flags such as start and peak
flare detection*	fldet	flare detection status for every minute
flare location	flloc	flare location
daily background	bkd1d	daily background and daily averages

* Most users should use the the flare summary instead of the flare detection product. See warning in Section 5.

2.1 Science Quality versus Operational XRS Data

The science quality L2 data products differ from the operational L2 products used in operations at SWPC in that they incorporate retrospective fixes that are not in the operational data as well as some recovered data that was missing in the real-time operational products. Also, this dataset uses the most recent calibrations. The science-quality L2 data products are created from the science quality L1b data. The operational L1b and L2 data, especially from the earlier dates, contain significant issues that are not retroactively corrected, and therefore should be used with great caution and not for scientific analysis.

2.2 Flare Magnitudes

A notable change between the GOES-R and previous GOES data is that the GOES-R XRS irradiances are provided in true physical units of W m^{-2} . The operational data prior to GOES-16 had scaling factors applied by SWPC to adjust the GOES 8-15 irradiances to match fluxes from GOES-7. The flare index was based on the operational irradiances, but to get true irradiances from the operational data, the scaling factors of 0.85 (for the XRS-A channel) and 0.7 (for the XRS-B channel) applied to GOES 8-15 had to be removed. There are no such scaling factors in the GOES-R XRS data; the provided irradiances are in true physical units.

The magnitude of a flare is defined by SWPC with a flare index that is based on the 1-minute average of the GOES operational irradiance in the XRS-B channel at the peak of the flare. Flare indices are denoted

by a letter and a number based on the log 10 peak irradiance of the flare (X: 10^{-4} W m $^{-2}$, M: 10^{-5} W m $^{-2}$, C: 10^{-6} W m $^{-2}$, B: 10^{-7} W m $^{-2}$, and A: 10^{-8} W m $^{-2}$). For instance, an M5 index is defined for a 5×10^{-5} W m $^{-2}$ peak irradiance, and an X2.5 index is defined as an irradiance level of 2.5×10^{-4} W m $^{-2}$ peak irradiance. The flare index is defined by the truncated (not rounded) irradiance; e.g., a flare with peak irradiance of 4.19×10^{-5} W/m 2 is an M4.1 flare, not an M4.2 flare. Because of the SWPC scaling factors in the pre-GOES-R data, flare indices for the earlier satellites were based on irradiances that were reported as 42% (1.0/0.7) smaller than for GOES-R (e.g., an X2.5 class flare reported operationally for GOES-15 will be an X3.6 class flare for GOES-R). Two XRS Level 2 (L2) products useful for flare detection are the event detection and event summary which provide flare peak irradiances, indices, and times.

A related note is that science-quality GOES 13-15 XRS reprocessed L1b and L2 data are now available. In the reprocessed GOES 13-15 data, the irradiances are provided in physical units (i.e., without the SWPC scaling factors) to match the GOES-R data. This earlier data is available from the GOES 8-15 tab at <https://www.ngdc.noaa.gov/stp/satellite/goes-r.html>.

2.3 XRS Response Functions

The responsivity for the GOES-16 XRS channels is shown in Figure 2. The response functions for all satellites, plots, a Readme, and an IDL code to read the data are available from the Documents link at <https://www.ngdc.noaa.gov/stp/satellite/goes-r.html>.

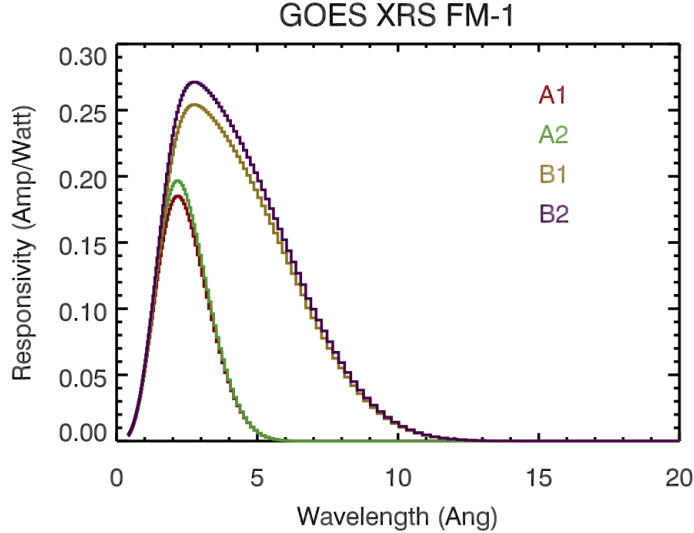


Figure 2: Response functions for the GOES-16 XRS channels.

2.4 Time

The time variable, $time[secs] = Time[UTC] - base_time[UTC]$, is an elapsed time in units of “secs since *base_time*” where $base_time = 2000-01-01\ 12:00:00[UTC]$ and was calculated without including leap seconds that occurred since 1 Jan 2000. Time stamps can be calculated by the user in Coordinated Universal Time (UTC) as

$$Time[UTC] = base_time[UTC] + time[secs] + n[secs] \quad (1)$$

where $n = 0$ for a time conversion function which ignores leap seconds (e.g., Python `cftime.num2date` or `netCDF4.num2date`) and $n = \text{number of leap seconds since } base_time$ if the function includes leap seconds. It should be noted that the reference epoch of “2000-01-01 12:00:00 UTC” is not the same as the J2000 epoch, because the latter is given in terrestrial time (TT) units which differ by more than a minute

from UTC. For a table of leap seconds, see <https://www.nist.gov/pml/time-and-frequency-division/time-realization/leap-seconds>.

2.5 Related New Data Products

Several related products are under development. Science-quality data is being reprocessed for GOES-1 through -15 with nearly identical file formats. Currently this project is complete for GOES-8 through -15, and will be completed for GOES-1 through -7 in 2024. This data, plots and a ReadMe is available from the 'GOES 1-15' tab at <https://www.ngdc.noaa.gov/stp/satellite/goes-r.html>.

A second new data product to be available in 2024 will be a flare report going back to GOES-1 in the 1970s. This composite product will list flares, flare times, magnitudes, and locations. There will be one entry per flare and both netcdf and ascii files will be provided. The flare report product will be on website in 2024.

3 1-second Irradiances Product

This product provides the XRS irradiances for the -A and -B channels along with a condensed set of quality flags. Values are provided for each detector (e.g., XRS-B1) and for the selected primary detectors (e.g., XRS-B). Additional variables include corrected currents for XRS-A2 and -B2, the roll angle, a factor to convert fluxes to 1 AU, and a yaw flip flag. Particle spikes, due to galactic cosmic rays, are flagged in the data.

Status flags are listed in Table 2.

Table 2: Status Flags for 1-sec data

Flag	Description
good.data	no other flags set
eclipse	Earth eclipse or lunar transit
particle_spike	particle spike
calibration	in flight calibration
off_point	satellite off-pointed
temperature_error	XRS temperature out of range
data_quality_error	signal too low/high or non-nominal condition
pointing_error	pointing uncalibrated or pointing error $> 0.4^\circ$; yaw flip in progress
invalid_mode	invalid L1b flags
missing.data	missing data
L0_error	L0 checksum error

Spikes are flagged with a simple equation with two terms which compare the signal to the current median irradiance and the noise level for the past hour. For an irradiance, I , a spike is defined as when

$$I_{flat} > 0.01 \cdot I + 1.05 \cdot |N_{min}| \quad (2)$$

where the flattened irradiance, $I_{flat} = I - median_{5\text{-point}}(I)$ and the noise $N_{min} = \min(N_{1hour}, N_{quiet})$. Here N_{1hour} is the lowest value (< 0) in I_{flat} during the previous hour, and N_{quiet} is the static quiet time minimum (also < 0) determined over multiple months. The flux term has an impact at high fluxes and ensures that spikes are significant at high fluxes. The noise term has an impact at low fluxes and during SEP events. This technique accounts for the fact that the signal has a relatively flat noise component which increases only when there is an SEP event.

4 1-minute Averages Product

This product contains the 1-minute averages of the 1-s cadence data. Data is flagged as good when it is not in an eclipse, does not have degraded pointing, is not a particle spike, and does not have the bad data flag

set. Status flags are listed in Table 3. The number of 1-s data points included in the average as well as the union of flags for the 1-s data that were excluded from the averages are also provided with the data.

Table 3: Status Flags for 1-min averages	
Flag	Description
good_data	neither eclipse flag nor bad data flag is set
eclipse	Earth eclipse or lunar transit
bad_data	large pointing error ($> 0.4^\circ$), missing data, or otherwise bad data
e_contam_significant	electrons contribute significantly to the observed X-ray flux.
e_correction_valid	valid electron correction
e_correction_invalid	invalid electron correction
e_correction_interp	electron correction is interpolated over a small gap in electron data
electron_correction_decay	electron correction is a decaying function

Electron contamination is removed in the 1-min-averaged data with a model based on a non-negative least squares fit of the GOES-R SEISS MPS-HI electron flux measurements (Boudouridis et al., 2020) to XRS-A1 and XRS-B1 data. No correction is applied to XRS-A2 and XRS-B2. Only XRS values below $2 \times 10^{-7} \text{ W m}^{-2}$ are included in the fit. Three X-ray averaged irradiance values are reported for each channel: the irradiance observed by the instrument (e.g., xrsb_flux_observed), the estimated electron contamination (e.g., xrsb_flux_electrons), and irradiance corrected for the electron contamination (e.g., xrsb_flux). For most purposes, the corrected flux should be used. The averaged irradiances are constrained to be above a minimum threshold of 10^{-9} W m^{-2} .

As shown in Table 3, there are five flags regarding the electron contamination correction. The valid and invalid flags are mutually exclusive. The correction method for doing the electron contamination removal is imperfect and sometimes when the amount of contamination is large, noticeable artifacts of the electron contamination remain in the corrected data. The e_contamin_significant flag indicates denotes when the estimated contamination is more than about 50% of the observed signal and thus may be significantly impacted by the imperfect correction; the exact threshold for this flag is given in the file metadata. Figure 3 shows the X-ray data for August 2020 for the XRS-B1 channel.

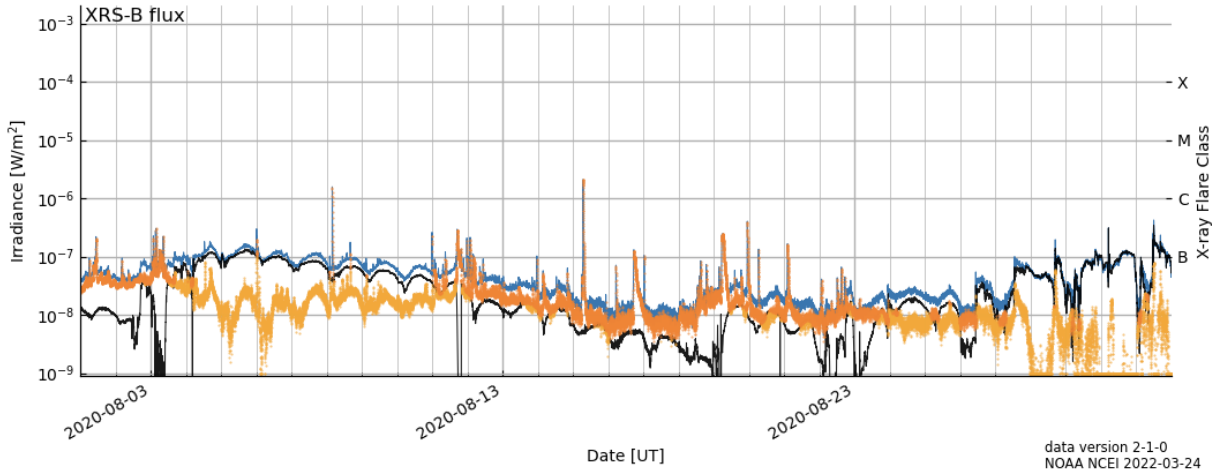


Figure 3: GOES-16 XRS-B1 observed signal (blue), estimated signal from electrons (black), and corrected XRS signal (dark and light orange) for the month of August 2020. Values in light orange indicate points where the e_contam_significant flag is set.

The electron correction interpolation and decay flags provide extra context. When there are missing SEISS electron measurements in the retrospective data, the correction factor is interpolated for gaps less than one hour and the electron_correction_interp flag is set in addition to electron_correction_valid. For missing

data in real time or gaps longer than one hour in retrospective data, the correction is a decaying function as shown in Figure 4. The `electron_correction_decay` flag will be set, along with `electron_correction_valid` for the first 60 minutes of decay. After 60 minutes of decay, it the `electron_correction_invalid` flag is set instead, even as the decay continues.

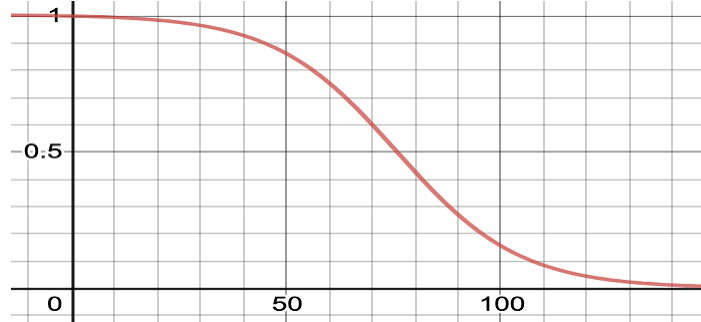


Figure 4: Decaying function applied to the electron contamination for gaps of greater than 1 hour. The decay function is $1.005/(1 + 0.005 \cdot e^{0.07 \cdot t})$ which is a logistic decay for time, t , in minutes.

5 Flare Summary and Flare Detection Products

The flare summary and detection products provide information on flares, including flare class, start and end times, integrated flux, and background flux based on 1-minute cadence XRS-B irradiances. The flare detection algorithm provides output every minute while the flare summary provides records only for the four most important states. Table 4 shows the available status flags for the two products.

Table 4: Status Flags for Flare Summary and Flare Detection Products

Flag	Description	Summary	Detection
MONITORING	There is no event in progress.		X
EVENT_START	A flare has just started.	X	X
EVENT_RISE	Flare has started but not reached its maximum.		X
EVENT_PEAK	Flare maximum.	X	X
EVENT_DECLINE	Flare has begun to decay.		X
EVENT_END	Flare has declined to 1/2 of flare maximum.	X	X
POST_EVENT	Flare declined to background.	X	X
IMPAIRED	Algorithm has insufficient data to determine status.		X

For most users, the flare summary product should be used and the flare detection product should not be used. The flare summary provides true time stamps for events. The flare detection algorithm must detect X-ray flares in real-time operations.

The flare detection product is used in real-time forecast operations, where minute-to-minute status information is the priority and also provides the input triggers to three other GOES-R L2 algorithms: XRS Flare Location, SUVI Bright Regions and SUVI Flare Location. The flare detection product is provided for users who wish to examine the algorithm behavior in detail retrospectively. The flare detection time stamps represent the time *when the algorithm detected an event*, such as the flare peak, rather than when the actual peak occurred. For two event types, flare start and flare peak, this results in flare detection time stamps that are delayed by several minutes. Flare end is also delayed by 0 to 2 minutes in the flare detection algorithm.

Figure 5 illustrates how the status flags are applied and the differences between the flare summary and flare detection time stamps. Details of the flare detection algorithm are provided in Appendix A.

A variable in the files, `sequential_flare_num`, provides the position of a flare in a sequence of flares, which can be useful when considering the meaning of the flare start, flare end, and integrated irradiances. For instance the integrated irradiance provided for a second flare includes the tail of the first flare. The `sequential_flare_num` variable is set to 1 for the first flare and set to 2, 3, etc. for subsequent flares.

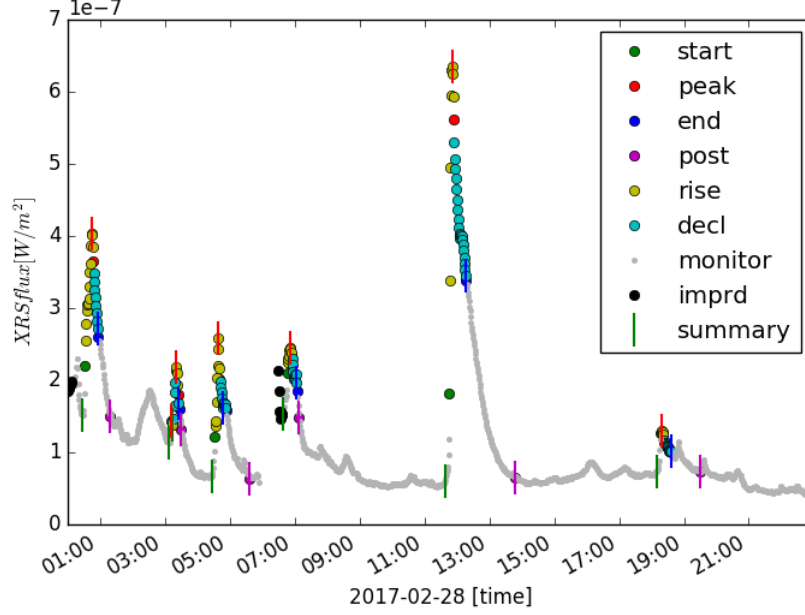


Figure 5: X-ray irradiance from GOES-16 on 28 February 2017. The dots color coded for the flare detection status at each minute. The vertical lines, with the same color codes, are at the actual event times as provided in the flare summary product. The EVENT_START and EVENT_PEAK true times (green and red vertical bars) occur prior to the detection of those event (green and red circles).

6 Flare Location Product

Flare location on the solar disk is determined based on the measurements from the high flux XRS-B2 quad diode detector (Chamberlin et al., 2009). Flare location is provided at EVENT_PEAK in four coordinate systems: Stonyhurst/heliographic (lon, lat), Carrington (lon, lat), heliocentric-radial (R , θ) and helioprojective Cartesian (x, y) coordinates. The solar P-angle and apparent solar angular radius are also provided. These coordinate systems are described by Thompson (2006). More details about the Flare Location Product calculation can be found in Appendix B.

This product was calibrated and validated with comparisons to flare locations from the Heliophysics Event Registry (HER; <https://www.lmsal.com/sungate/>). The HER data is included in the Heliophysics Events Knowledgebase (HEK; <https://www.lmsal.com/hek/index.html>). As shown in Table 5, the median errors are $\lesssim 1$ arcmin for C class and above flares.

Table 5: Statistics for the XRS Flare Location Product*

Class	GOES-16		GOES-17		GOES-18	
	No. of Flares	Median Error [arcmin]	No. of Flares	Median Error [arcmin]	No. of Flares	Median Error [arcmin]
X	27	0.81	11	0.72	14	0.99
M	584	0.50	225	0.47	403	0.54
C	5378	1.04	2493	0.97	3233	1.13
B	3077	3.57	2258	3.47	110	2.38
All (C-X)	5989	0.95	4451	0.91	3650	1.05

* For flares between 2017-02-09 to 2024-01-01 for GOES-16, 2018-06-01 to 2023-01-09 for GOES-17, and 2022-09-08 to 2024-01-01 for GOES-18.

Because the flare location algorithm requires an estimate of the solar irradiance background, it works best for flares that do not overlap a previous flare. For a non-initial flare in an overlapping sequence of

flares (i.e., when *sequential_flare_num* > 1), it is challenging to get a good estimate of the decaying solar background from the previous flare.

7 Daily Background Product

This product provides daily average irradiances and daily backgrounds for XRS-A and -B. The algorithm uses hourly and 8-hour minima of the 1-minute averages to determine the daily background values.

The algorithm is designed to be consistent with the logic from the former GOES XRS daily background algorithm originally developed by Dave Bouwer in 1981. Using the observation that most major X-ray flares last at most about 8 hours, and that the algorithm is most applicable in describing mid-to-long-term coronal variations on time scales of weeks to years, an approximation of coronal background variations for statistical time series comparisons to other solar indices (e.g., F10.7 cm radio emissions) could be useful in describing solar active region evolution and the solar cycle. An example of the daily background product is shown in Figure 6. The details of the daily background algorithm are given in Appendix C.

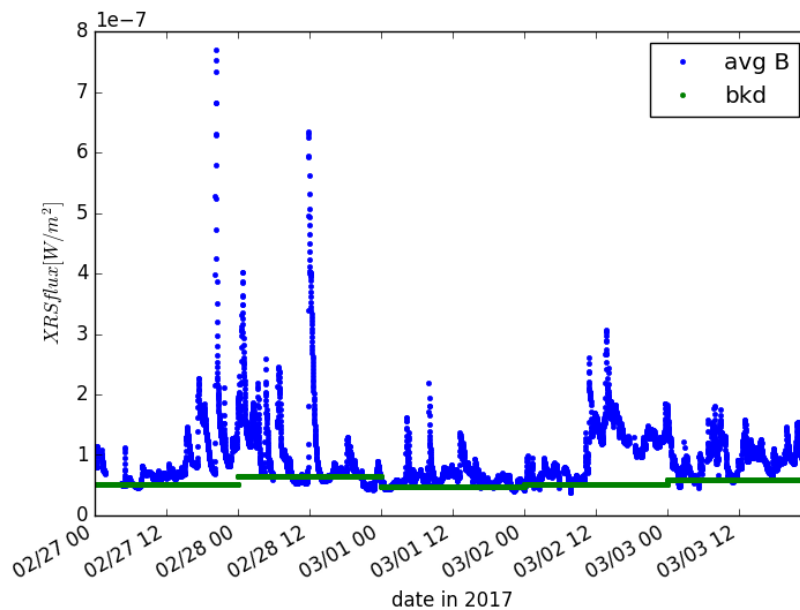


Figure 6: Daily background (green) and 1 minute XRS averages (blue) over 5 days.

8 Plots

Monthly summary plots are provide for both the science-quality and operational 1-minute averaged data. The files contain plots for each of the four detectors (A1, B1, A2, and B2). Traces are shown for the observed and electron-corrected irradiances as well as the estimated electron contamination. An example of the summary plots is shown in Figure 7 for September 2017, a period with X-class flares.

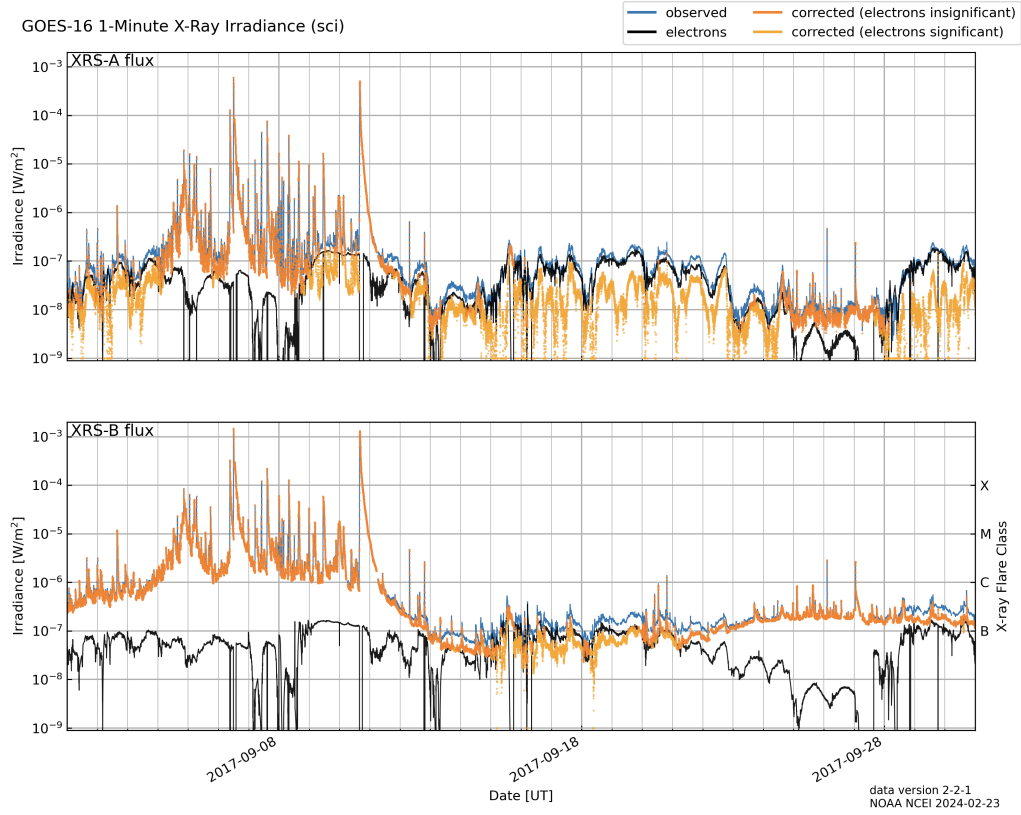


Figure 7: Example monthly summary plot showing X-class flares in GOES-16 XRS science-quality data for September 2017.

9 Acknowledgements

We thank the following people for their work on the development and validation of the L2 algorithms: Dave Bouwer, Thomas Eden, Frank Eparvier, Brooke Kotten, James Mothersbaugh III, Steve Mueller, James Negus, Laurel Rachmeler, Alysha Reinard, Kent Tobiska, Rodney Viereck, Donald Woodraska, and Thomas Woods. We thank Tom Woods and Don Woodraska for the responsivity values, plots, and code. We thank Kevin Hallock, Ann Marie Mahon, Josh Riley, and Pamela Wyatt for data processing and data management of this data. We thank Brian Kress, Juan Rodriguez and Andrew Wilson for assistance with the particle data.

10 References

- Boudouridis, A., J.V. Rodriguez, B.T. Kress, B.K. Dichter, and T.G. Onsager (2020). Development of a Bowtie Inversion Technique for Real-time Processing of the GOES-16/-17 SEISS MPS-HI Electron Channels. *Space Weather*, 18, e2019SW002403. <https://doi.org/10.1029/2019SW002403>
- Chamberlin, P. C., F. G. Eparvier, A. R. Jones, and T. N. Woods, Next Generation X-Ray Sensors (XRS) for the NOAA GOES-R Satellite Series, *SPIE Proc.*, 7438-23, 2009. <https://doi.org/10.1117/12.826807>
- Garcia, H. A. (1994), Temperature and emission measure from GOES soft X-ray measurements, *Sol. Phys.* 154, 275.
- Machol, J., F. Eparvier, R. Viereck, D. Woodraska, M. Snow, E. Thiemann, T. Woods, W. McClintock, S. Mueller, T. Eden, R. Meisner, S. Codrescu, S. Bouwer, and A. Reinard (2020), GOES-R Series Solar X-ray and Ultraviolet Irradiance. In S. Goodman, T. Schmit, J. Daniels, R. J. Redmon) (Eds.), *The GOES-R Series: A New Generation of Geostationary Environmental Satellites* (pp. 233-242), Amsterdam: Elsevier. <https://doi.org/10.1016/B978-0-12-814327-8.00019-6>
- Neupert, W.M. (1968). Comparison of Solar X-Ray Line Emission with Microwave Emission during Flares, *Astrophys. J.* 153, L59. <https://doi.org/10.1086/180220>
- Thomas, R.J., R. Starr, and C.J. Crannell (1985). Expressions to determine temperatures and emission measures for solar X-ray events from GOES measurements. *Solar Phys.* 95, 323-329. <https://doi.org/10.1007/BF00152409>
- Thompson, W.T. (2006). Coordinate systems for solar image data. *A&A*, 791-803. <https://doi.org/10.1051/0004-6361:20054262>
- White, S.M., R.J. Thomas and R.A. Schwartz (2005). Updated expressions for determining temperatures and emission measures from GOES soft X-ray measurements, *Solar Phys.* 227, 231-248. <https://doi.org/10.1007/s11207-005-2445-z>
- Woods, T. N., P. C. Chamberlin, W. K. Peterson, R. R. Meier, P. G. Richards, D. J. Strickland, G. Lu, L. Qian, S. C. Solomon, B. A. Iijima, A. J. Mannucci, and B. T. Tsurutani (2008), XUV Photometer System (XPS): Improved irradiance algorithm using CHIANTI spectral models, *Solar Physics*, 249, <https://doi.org/10.1007/s11207-008-9196-6>

Appendix A Flare Detection Algorithm

A.1 Flare Detection Algorithm

One of the challenges in developing the event detection algorithm was mitigating the effects of signal noise which can result in false-positives or inaccurate identification of the flare peak or end. Because the block of data examined each moment ("data-frame") is small (generally less than ten points of 1-minute data so as not to include multiple flares), accurate statistics are difficult to achieve. In most cases, the algorithm uses a variety of criteria including an exponential fit to determine that a flare has begun.

The recent background flux level is used both for the exponential fit for the flare rise and for determining the flare end. The best choice for the background can be difficult to select; for example, an hourly average or a shorter time interval could be used to estimate a background. Also, significant signal noise or rapidly repeating flares can result in a too high background estimate, significantly hindering the ability of an algorithm to detect or characterize a flare. By fitting an exponential model to the initial rise of a flare, and using its minimum value, a more accurate background can be estimated that is less susceptible to rapid flaring or signal noise. However, this background can still be in error by up to about $\pm 20\%$ in cases where the pre-flare data has significant signal noise or the flare rises to its peak in several minutes.

Figure 8 presents a flow chart outlining the sequence of operations for the algorithm. Fill values are used whenever a calculation cannot be performed due to missing data. Section A.2 presents the algorithm steps.

A.2.1 (Steps 1-6) Prepare data and do simple comparisons

1. **Read** next 1-minute data point with *flux* and *curr_time*.
2. **Initialize** variables as needed.
 - Set *prev_status* = **IMPAIRED**.
 - Set all fluxes to *bad_flux*.
 - Set *sequential_flare_num* = 0.
 - Set *prev_flare_ended* = 0 **TRUE**.
 - Set *time_of_prev_peak* = 1 Jan 1970.
3. **Read** in recent data and current parameters.
4. Create the real time "raw data frame" of raw fluxes, X_i , numbered from 0 to $N-1$, where $N = \text{frame_mins}$. Put most recent flux in the final element of frame. Transfer fluxes from the previous frame into the current frame, leaving the last element available for the new data point. Any gaps in time or differences in array length will result in those elements in the current frame filled with *bad_flux*.
5. If there is any *bad_flux* in the frame, then set *status* = **IMPAIRED** and proceed to "Final steps".
6. For raw fluxes X_i where i is in the first $N-2$ values, **calculate the *standard_dev*** as

$$\sigma = \sqrt{\sum_i (\bar{X} - X_i)^2 / \bar{X}}$$

where \bar{X} is the mean. Also, **smooth** the full data frame with a small, simple boxcar filter over *n_smooth* points to mitigate noise and reduce false positives. This produces a new data frame of x_0 to x_{n-1} , where the number of elements is $n = N - (n_smooth - 1)$. Typically a 3-minute window is adequate. To simplify timing, the filter width should be an odd number.

7. If $x_{n-1} < \text{min_flux_good}$ then set *status* = **IMPAIRED** and proceed to "Final steps".

A.2.2 (Steps 8a-f) Check for start of flare

At this point, there is a full frame of good data. If the status is not currently in a flare, then the following steps are followed to check if there is a start of a flare. The status is already in a flare event if *prev_status* = *not*(**MONITORING**, **IMPAIRED**, **EVENT_END** or **POST_EVENT**).

8. If *prev_status* did not indicate a flare event, then proceed through Steps a-j.
 - a. If $x_{n-1} < \text{background}$ then set *status* = **POST_EVENT**, set *background* = -999.0, and proceed to "Final steps". The background value is set low to ensure that **POST_EVENT** is only set once.
 - b. If **flux is high** and previously points were low, i.e., $(X_{n-1} > \text{high_flux})$ AND $\max([X_0, \dots, X_{n-2}]) < (R2 - \text{min_num_std} \cdot \sigma)$, then set *status* = **EVENT_START**, set the pre-flare background to the minimum smoothed flux in frame and proceed to "Final steps".
 - c. Set *status* = **MONITORING**.
 - d. If the flux is inadequate for an inflection point, $x_{n-1} < \text{min_inflection_flux}$, then proceed to "Final steps".
 - e. If an **inflection point** has not been reached in the slope of the data frame using the second derivative of the data frame, then proceed to "Final steps". The inflection point is at $\max(d^2x/dt^2)$. To know that this is the inflection point, and not just part of an increasing slope, requires that this point not be the final point within the frame; so, this routine checks the penultimate second derivative. With n time steps of 1 minute (i.e., $dt = 1$), there are $n - 1$ first derivatives in the data frame and $n - 2$ second derivatives which we calculate as $dx_i = x_{i+1} - x_i$, for $i = 0$ to $n - 1$ and $d^2x_j = dx_j - dx_{j-1}$, for $j = 0$ to $n - 2$.

- f. If flux data has not risen by at least a minimum number of **standard deviations**, then proceed to "Final steps". Calculate the difference in the mean of the first 3 data points versus the mean of the last 3 data values in the frame. There is a potential flare if

$$x_{n-1} - x_0 > \text{min_num_std} \cdot \sigma. \quad (3)$$

- g. Fit to an **exponential function**. The fit for the impulsive rise of the flare is to the function:

$$\Phi_{imp}(t) = a \cdot e^{b \cdot t} + c \quad (4)$$

where $t > 0$. Determine the *correlation_coef* and set *temp_background* to minimum of the fitted exponential function (value at $i = 0$).

Proceed to "Final steps" in any of the following cases:

- i. The **rise is inadequate** if $x_{n-1}/\text{temp_background} < \text{min_ratio_to_bkd}$ or $a < 0$ or $b < 0$.
- ii. The exponential **fit is bad** if $\text{correlation_coef} < \text{min_corr_coef}$.
- iii. The exponential function is **not increasingly concave** as it should be. The exponential fit determines that the flux is increasing (i.e., $a > 0$ and $b > 0$ in Equation 4), and so in this step it is only necessary to verify that the function is concave. A function is concave if the second derivative is > 0 . The second derivative of Equation 4, is
$$d^2\Phi_{imp}(t)/dt^2 = a \cdot b^2 \cdot e^{b \cdot t}. \quad (5)$$

The fit function is concave when $d^2\Phi_{imp}(t)/dt^2 > 0$; i.e., when $a > 0$. (Redundant with Step i.)
- iv. The **SNR is not adequate** if the mean of the last 3 points of the exponential function estimate lies a factor less than *min_exp_rise_factor* above the mean of the first 3 data points of the exponential fit.
- h. Set *status* = EVENT_START. Set the pre-flare background to *temp_background*. Set *mins_since_event* to the number of minutes (> 0) between the time of the minimum flux and the end of the frame. Proceed to "Final steps".

A.2.3 (Steps 9a-c) Rising flare

9. If **flare is rising** (*prev_status* = EVENT_START or EVENT_RISE) then proceed through Steps a-c to look for a peak:
 - a. There was a **flare maximum** if the maximum flux in the last *peak_frame_mins* of the frame is the first point in this peak frame.
 - b. If there was no flare max then, set *status* = EVENT_RISE and proceed to "Final steps".
 - c. In this case, a **flare max** has occurred. Set *status* = EVENT_PEAK, *peak_flux* = maximum flux, *mins_since_peak* = *peak_frame_mins* - 1, and *peak_time* = *curr_time* - *mins_since_peak*. Proceed to "Final steps".

A.2.4 (Steps 10a-b) Declining flare

10. If **flare is declining** (*prev_status* = EVENT_PEAK or EVENT_DECLINE) then proceed through Steps a-e to check for a flare end or a new flare start:
 - a. If **end of flare**, then set *status* = EVENT_END and proceed to "Final steps". The event end is defined as when

$$\{\text{median}([X_{n-3}, X_{n-2}, X_{n-1}]) - \text{background}\} \leq (\text{peak_flux} - \text{background})/2. \quad (6)$$

Set *mins_since_event* = *curr_time* - *time_i* for first i where $(X_i - \text{background}) \leq (\text{peak_flux} - \text{background})/2$.

This is also the timestamp for the flare summary product EVENT_END. Note: the POST_EVENT flag is set in Step 8a if $\text{flux} < \text{background}$.

- b. Set *status* = EVENT_DECLINE
- c. If the elapsed time since the peak is too short to start looking for another flare (*curr_time* – *peak_time* < *min_time_after_peak*), then proceed to "Final steps".
- d. If a new flare has begun, then set *status* = EVENT_START, set the pre-flare *background* to the minimum non-smoothed flux since the peak, and set *mins_since_event* = *curr_time* – (time of this minimum flux).

A new flare is indicated if either (1) the **flux is high** ($X_{n-1} > \text{high_flux}$) and *peak_flux* < *high_flux*, or (2) the smoothed flux has risen by at least a minimum number of standard deviations. In the second case, in the subset of the current frame where the time is at least *mins_since_peak* minutes have elapsed since the peak, the index *j* of the minimum flux is found. There is a flare start if:

$$x_{n-1} - x_j > \text{min_num_std} * \sigma. \quad (7)$$

- e. Proceed to "Final steps".

A.2.5 (Steps 11a-e) Final steps to exit

- 11. Final steps to exit.

- a. If *status* = IMPAIRED or POST_EVENT, then set *background* = *background_reset* so that a subsequent POST_EVENT will not be declared.
- b. If *status* = EVENT_START, then

$$\text{integrated_flux}[J/m^2] = \frac{60 \text{ s}}{\text{1-min average}} \cdot \sum_{n-1-\text{mins_since_start}}^{n-1} x_i[W/m^2]. \quad (8)$$

- c. If *status* = EVENT_RISE, EVENT_PEAK, EVENT_DECLINE, or EVENT_END, then add to the integrated flux:

$$\text{integrated_flux}[J/m^2] += \frac{60 \text{ s}}{\text{1-min average}} \cdot x_{n-1}[W/m^2] \quad (9)$$

- d. if (*prev_flare_ended* = TRUE) or (!(*status* = START or RISING) and (*curr_time* – *time_of_prev_peak*) > 90 minutes), then set *sequential_flare_num* = 0.
- e. If *status* = EVENT_START, then set *sequential_flare_num* = *sequential_flare_num* + 1 and *prev_flare_ended* = FALSE.
- f. If *status* = EVENT_PEAK, then set *time_of_prev_peak* = *curr_time*.
- g. If *status* = EVENT_END or MONITORING or IMPAIRED or POST_EVENT, then set *prev_flare_ended* = TRUE.
- h. Write a real time flare detection record with *curr_time*, *status*, and x_{n-1} . Also write out the integrated flux if *status* = EVENT_START, EVENT_RISE, EVENT_PEAK, EVENT_DECLINE, or EVENT_END.
- i. Write a flare summary record if *status* = EVENT_START, EVENT_PEAK, EVENT_END, or POST_EVENT.

A.3 Algorithm Inputs

For the flare detection algorithm the input data is the XRS-B fluxes from the L2 1-minute average files (xrsf-l2-avg1m). Some of the configurable inputs for the algorithm are given in Table 6. Some of the variables used within the algorithm are given in Table 7.

Table 6: Configurable inputs for the flare detection algorithm.

Parameter	Description	Example	Units
bad_flux	fill value for bad fluxes	—	—
frame_mins	data frame size	9	mins
high_flux	threshold for expedited flare declaration	5e-5	W/m^2
max_iter_exp_fit	maximum number of iterations	30	—
min_corr_coef	minimum correlation coefficient	0.925	—
min_exp_rise_factor	minimum ratio of end of fit to start of fit	1.225	—
min_flux_good	minimum flux threshold below which status is IMPAIRED	1e-9	W/m^2
min_inflection_flux	minimum flux for inflection point to be an EVENT_START	1e-7	W/m^2
min_num_std	minimum number of standard deviations above background	1	—
min_ratio_to_bkgd	minimum ratio to background for event start	1.225	—
min_time_after_peak	minimum time after an event start before next event start	8	mins
n_smooth	size of smoothing window	3	—
peak_frame_mins	size of data frame used to determine event peak	7	—

Table 7: Variables within the flare detection algorithm.

Variable	Description
background	most recent background flux
background_reset	value < 0 to reset background
curr_time	time of current record
event_time	time of last event
integrated_flux	integrated since last EVENT_START
mins_since_event	used for EVENT_START and EVENT_END
mins_since_peak	minutes since last EVENT_PEAK
peak_flux	most recent peak flux
prev_status	status of previous minute
peak_time	time of last peak
prev_flare_ended	True/False; Did previous flare reach EVENT_END?
sequential_flare_num	number of flare in current flare sequence, ≥ 0
standard_dev	standard deviation of n-2 smoothed frame elements
status	current status
time_of_prev_peak	time of previous peak

Appendix B Flare Location Algorithm

The mathematical formulation of the Flare Location Algorithm is described in this appendix. As input, this algorithm uses the L2 1-minute XRS data product and the Flare Summary product. The Flare Location Algorithm is triggered when a flare EVENT_PEAK is flagged in the Flare Summary product, and calculates a location using the quad diode intensities in the 1-minute product.

The flare location is calculated based on the center-of-mass of the flare intensity observed on the XRS-B2 quadrant photodiodes. The four quadrant photodiodes in the XRS-B2 detector are ordered clockwise as shown in Figure 9.

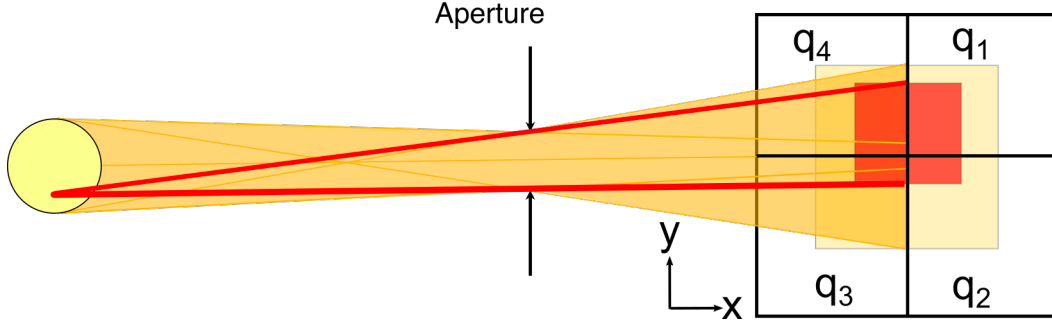


Figure 9: Sketch of the XRS-B2 quad diode on the right with the quadrants labeled and a flaring Sun on the left. The background light from the Sun is represented in yellow and the light from the flare in red. The algorithm calculates the location of the flare as the center-of-mass of light from the flare.

The first step of the calculation is to isolate the flaring light by subtracting a background solar brightness from each quadrant so that $Q_i = q_i - b_i$ where q_i is the corrected current and b_i is the background corrected current for quadrant i . The background for each quadrant is the average of all corrected currents below the EVENT_START current for the 7 minutes prior to EVENT_START. If no values meet this criteria, then the corrected current at EVENT_START is used as the background.

The measured center-of-intensity of the background-subtracted flare intensity is then calculated in detector coordinates:

$$x_{det} = \frac{(Q_1 + Q_2) - (Q_3 + Q_4)}{\sum_{i=1}^4 Q_i} \quad y_{det} = \frac{(Q_1 + Q_4) - (Q_2 + Q_3)}{\sum_{i=1}^4 Q_i} \quad (10)$$

where the detector coordinates are in the range of $-1 < x < 1$ and $-1 < y < 1$.

The location is then converted from detector coordinates (x_{det}, y_{det}) to Heliocentric Cartesian coordinates (x_{XRS}, y_{XRS}) in arcmin. This involves a rotation correction by an angle α' to align solar north with x_{det} , and has several parameters associated with both static and dynamic offsets in pointing, roll, and field-of-view.

$$x' = x_{det} + x_{offset} \quad y' = y_{det} + y_{offset} \quad (11)$$

$$x_{XRS} = (x' \cos \alpha' - y' \sin \alpha') F_x \quad y_{XRS} = -(x' \sin \alpha' + y' \cos \alpha') F_y \quad (12)$$

$$\alpha' = P_{ang} + \alpha_{roll} \quad (13)$$

Here, x_{offset} and y_{offset} are static offsets applied to the detector coordinates. Physically they can be interpreted as small offsets between the satellite pointing and the center of the field-of-view of the detector. The solar P-angle (P_{ang}) is the angle between the celestial north pole and the solar rotational north pole and can be calculated from solar ephemeris data; it is provided in the flare location data product. The spacecraft roll angle (α_{roll}) is the measured roll angle of the satellite relative to the celestial pole, and is provided in the

1-minute average XRS data product. The overall correction angle, α' , is measured counterclockwise. The angles F_x and F_y are the half-fields-of-view of the XRS-B2 detector in the x and y directions.

For each satellite, the four adjustable parameters in the coordinate transformation, x_{offset} , y_{offset} , F_x , and F_y , were optimized simultaneously with a Monte Carlo method. A set of known flare locations for M- and X-class flares, as reported in the Heliophysics Event Registry (HER), was used for the “true” locations of the flares, and the Monte Carlo method was used to determine the set of parameter values that minimized the difference between the flare locations as reported in the HER and calculated for XRS. Flares that overlapped in time, as defined by *sequential_flare_num* > 1, were excluded from these calculations. The best-fit parameters used in the flare location algorithm are listed in Table 8.

Table 8: Best-fit parameters* for the XRS Flare Location algorithm

Free Parameter	GOES-16	GOES-17	GOES-18
x_{offset} [detector units]	0.00490	-0.03473	-0.0430
y_{offset} [detector units]	-0.01375	0.01997	-0.0109
F_x [arcmin]	86.24	85.66	84.21
F_y [arcmin]	84.72	82.95	81.53

* Analysis periods to determine parameters were 2019-01-24 to 2023-11-15 for GOES-16, 2019-01-24 to 2023-01-09 for GOES-17, and 2022-09-08 to 2023-11-09 for GOES-18.

Appendix C Daily Background Algorithm

This algorithm creates a daily X-ray background irradiance from the XRS-B 1-minute irradiances. If there is no data to be averaged, then a fill value is output for the irradiances and the flag is set to bad data. Figure 10 presents a flow chart outlining the sequence of operations for the algorithm. Fill values are used whenever a calculation cannot be performed due to missing data.

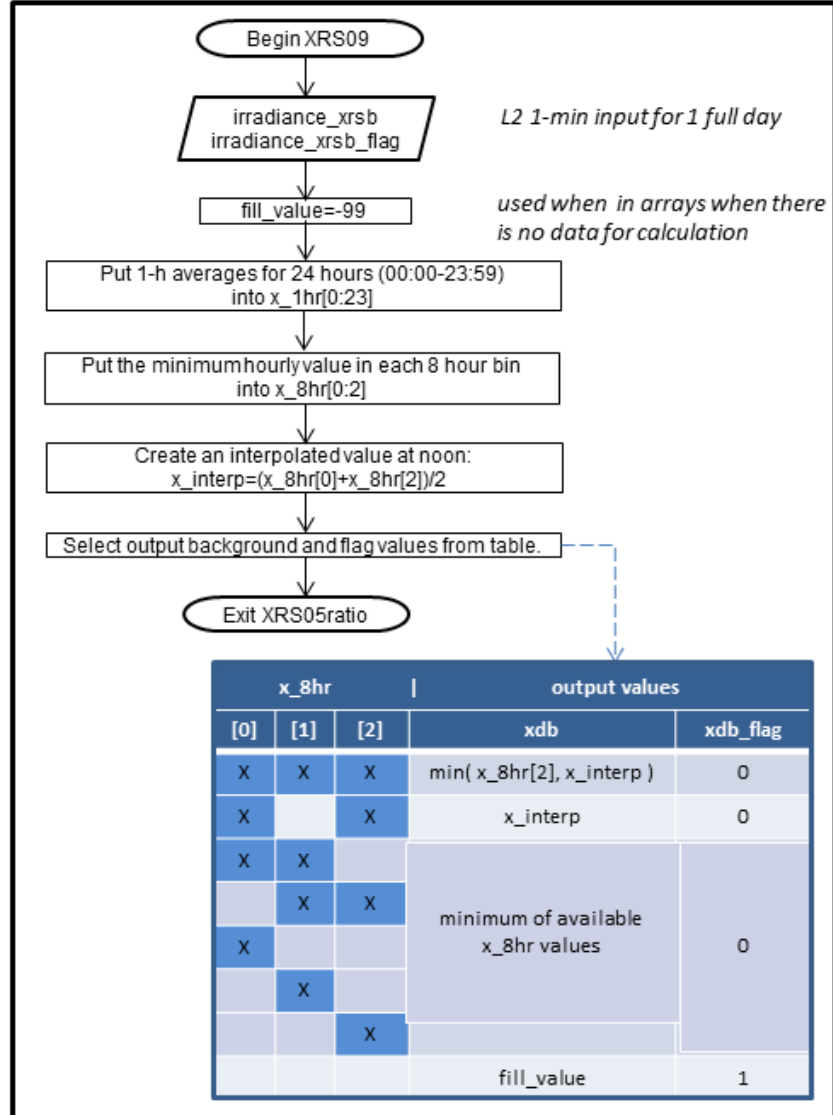


Figure 10: Flowchart of daily background algorithm.

The sequence of operations is:

1. Calculate hourly averages from XRS-B (0.1-0.8 nm) one-minute fluxes if there is at least 1 valid data point for the hour.
2. Divide 24 hourly averages into three equal blocks of 8 hours, x_8hr: e.g., 00-07, 08-15, and 16-23.
3. Calculate the minimum hourly average for each of the 3 blocks.
4. Perform a simple average of the minima of the 2 outer blocks for an interpolated minimum at noon.

5. Set the X-ray daily background (xdb) as the mid-day minimum if at least one of the three bins has good data. Set the xdb_flag=0.
 - a. If all three 8-h blocks have good data, select the lower minimum from either the middle bin or the interpolated noon bin.
 - b. If the middle block has no data, select the interpolated minimum.
 - c. When either the first or third block does not have data, select the lower of the two remaining blocks.
 - d. If only one block has data, use its value.
6. If no blocks have good data, set xdb to the fill value and set the xdb_flag=1 for missing data.